Advanced Review

Physics and chemistry of oxidation of two-dimensional nanomaterials by molecular oxygen

Gaoxue Wang,[1†] Ravindra Pandey[1†*] and Shashi P. Karna[2†]

The discovery of graphene has inspired extensive interest in two-dimensional (2D) materials, and has led to synthesis/growth of additional 2D materials, generally referred to as 'Beyond Graphene'. Notable among the recently discovered exotic 2D materials are group IV elemental monolayers silicene and germanene, group V elemental monolayer phosphorene, and binary monolayers, such as hexagonal boron nitride (*h*-BN), and molybdenum disulfide (MoS_2). Environmental effect on the physical and chemical properties of these 2D materials is a fundamental issue for their practical applications in devices operating under ambient conditions, especially, exposure to air often leads to oxidation of nanomaterials with significant impact on the functional properties and performances of devices built with them. In view of its importance, we present here a review of the recent experimental and theoretical studies on the oxidation of 2D materials focusing on the relationship between the oxidation process and the energy values which can be calculated by first principles methods. The complement of experiments and theory facilitates the understanding of the underlying oxidation process in terms of cohesive energy, energy barrier to oxidation and dissociation energy of oxygen molecule for 2D materials including graphene, silicene, germanene, phosphorene, *h*-BN, and MoS_2.

How to cite this article:
WIREs Comput Mol Sci 2016. doi: 10.1002/wcms.1280

INTRODUCTION

The discovery of graphene[1,2] has inspired extensive interest in two-dimensional (2D) materials due to their unique properties and promising applications in electronics and optoelectronics, including transistors,[3–8] sensors,[9–13] energy storage and conversion devices,[14–20] and light-emitting devices.[21–27] Such wide range of applications has led to a fundamental question of the environmental effect on the physical and electronic properties of 2D nanomaterials. Of particular importance is the oxidation of materials in air, which can have significant impact on the functional properties and the performance of the devices built with them. Atomically thin 2D nanomaterials may exhibit high sensitivity to oxidation due to their large surface area. Additionally, oxidation plays important role in large scale synthesis of graphene.[28–30]

Oxidation of 2D nanomaterials strongly depends on their bonding characteristics, which can be distinctly different from one to another. For example, graphene is found to be stable against oxidation under ambient conditions.[1] However, silicene, the other group IV elemental monolayer, is found to quickly oxidize in air.[31] Phosphorene, a recently isolated group V elemental monolayer, is found to be chemically unstable in air.[32–34] Oxidation of 2D materials in ambient conditions can therefore present challenges in synthesis, characterization, and integration in active devices. Atomically thin 2D

†These authors contributed equally to the review of this paper.

*Correspondence to: pandey@mtu.edu

[1]Department of Physics, Michigan Technological University, Houghton, MI, USA

[2]Weapons and Materials Research Directorate, US Army Research Laboratory, Aberdeen Proving Ground, MD, USA

Conflict of interest: The authors have declared no conflicts of interest for this article.

nanomaterials exhibit high sensitivity to oxidation due to their large surface area, unsaturated valencies, and atomic-level defects among other factors. Thus, a detailed study of oxidation of 2D nanomaterials is of particular importance, both for gaining an enhanced understanding of their fundamental properties and for their potential applications in devices.

Since the field of 2D nanomaterials is growing rapidly, it is a daunting task to present a detailed review on all recently discovered materials. However, with a view to capture the underlying physics and chemistry, we present here a comprehensive review of the recent experimental and theoretical studies on oxidation of selected number of 2D materials that have attracted attention for their potential applications in nanotechnology. The considered 2D materials in this review include the group IV elemental monolayers, namely graphene, silicene, and germanene; the group V elemental monolayer, phosphorene; and binary monolayers, hexagonal boron nitride (*h*-BN), and molybdenum disulfide (MoS_2).

THEORY

Theoretical studies on oxidation of 2D nanomaterials have been mainly based on density functional theory (DFT) which has been a popular approach with remarkable success in addressing issues related to physics and chemistry of materials.[35] DFT calculations can be successfully used to investigate atomic-level interaction of oxygen molecule with 2D materials, in addition to accurately establishing stable geometry and electronic structure, thus making it possible to relate the structure and chemistry of the materials to the oxidation process. In general, oxidation of 2D materials can be understood in terms of the energy barrier ($E_{barrier}$) to the transition state, and the dissociation energy (E_{diss}) of O_2 during the process. These energy values in turn depend on the strength of chemical bonds in the materials, which is related to the cohesive energy (E_{coh}). It is now possible to calculate the energy parameters $E_{barrier}$, E_{diss}, and E_{coh} with an accuracy of few meV with the use of the state-of-art DFT methods.

Cohesive Energy of 2D Materials

Cohesive energy, E_{coh}, is defined as the energy released after the formation of a material from its constituting atoms and can be calculated as, $E_{coh} = (N \times E_{atom} - E_{total})/N$, where E_{total} is the total energy of the 2D material, E_{atom} is the energy of a constituting atom, and N is the number of constituting atoms. E_{coh} is related to the strength of chemical bonds within the 2D lattice. The larger the value of E_{coh}, the stronger the chemical bonds in the lattice. The values of E_{coh} of selected 2D materials obtained from DFT calculations are listed in Table 1. Note that the cohesive energy of some of the materials spans a wide range (around 1 eV) due to the use of different functional forms in DFT calculations.

Among the studied 2D materials, graphene and *h*-BN have the largest value of E_{coh} (greater than 7.0 eV/atom[36–38,51,52]) originating from their planar structure with strong sp^2 hybridized atoms forming σ bonds and the out-of-plane π bonds. Therefore, graphene and *h*-BN show good stability and resistance toward oxidation at ambient conditions. Silicene and germanene have relatively smaller value of E_{coh} in the range of 4.2–5.2[38,42,43] and 3.4–4.2 eV/atom,[38,42] respectively, due to their buckled structure with slightly weaker sp^2–sp^3 hybridized bonds. Therefore, both silicene and germanene are found to be sensitive to O_2.[31] The cohesive energy of phosphorene is 3.3–3.8 eV/atom,[47,48] which is about half the value for graphene or *h*-BN. Enhanced sensitivity of phosphorene to oxygen is confirmed by experiments, which have demonstrated rapid degradation of this material.[32,33,57,58] Overall, the cohesive energy is a general indicator of the strength of chemical

TABLE 1 | Calculated Lattice Constant, Cohesive Energy (E_{coh}), Energy Barrier ($E_{barrier}$), and the Dissociation Energy (E_{diss}) of O_2 During Oxidation of 2D Materials

2D Monolayer	Lattice Constant (Å)	E_{coh} (eV/atom)	$E_{barrier}$ (eV)	E_{diss} (eV)
Graphene	2.46	7.7–7.9[36–38]	2.2–2.7[39–41]	0.7–2.2[39–41]
Silicene	3.87	4.2–5.2[38,42,43]	0.0[44]	–4.0 to –5.4[44]
Germanene	4.04	3.4–4.2[38,42]	0.6[45,46]	–2.3 to –2.5[45,46]
Phosphorene	4.62, 3.30	3.3–3.8[47,48]	0.1–0.5[49,50]	–4.0 to –4.5[49,50]
h-BN	2.51	7.1–7.9[51,52]	1.2–2.6[53]	1.1–2.2[53]
MoS_2	3.19	5.0–5.1[54,55]	1.6[56]	—

E_{coh} and $E_{barrier}$ were calculated with either the Generalized Gradient Approximation with the Perdew–Burke–Ernzerhof functional (GGA-PBE) or the Local Density Approximation (LDA-DFT). The lattice constants were calculated at GGA-PBE level of theory.

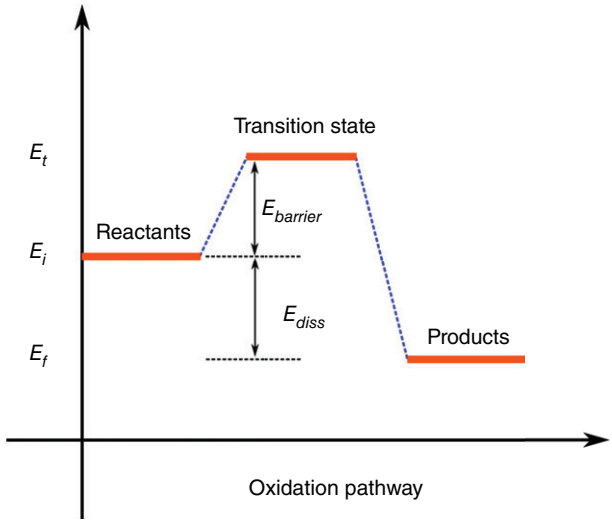

FIGURE 1 | A schematic illustration of the oxidation pathway on 2D materials.

bonds within the 2D material, thus its stability toward oxidation.

Energy Barrier and Dissociation Energy During Oxidation

In addition to the cohesive energy, the energy barrier (E_{barrier}) and the dissociation energy (E_{diss}) are quantities directly related to oxidation of the material which involves multiple reaction steps; the overall reaction rate is determined by the slowest step referred to as the rate-determining step for the process in air. Figure 1 depicts a simplistic schematics and not really suggestive of quantitative process associated with dissociation of an oxygen molecule on 2D materials. Here, E_i is the energy of the reactants including the pristine 2D material and an O_2 molecule, E_t is the energy of the transition state, and E_f is the energy of the system after the dissociation of O_2 on the 2D lattice. The energy barrier (also known as the activation energy) during oxidation process is calculated as $E_{\text{barrier}} = E_t - E_i$, and the dissociation energy is $E_{\text{diss}} = E_f - E_i$. We note that E_{barrier} and E_{diss} are related to the fundamental interaction of O_2 with 2D materials, thus providing insightful information to their stability against oxidation.

The energy barrier, E_{barrier} determines how fast oxidation of 2D materials could occur. According to the Arrhenius relationship,[59] the reaction rate $K = Ae^{-E_{\text{barrier}}/k_BT}$, where A is a preexponential term, k_B is the Boltzmann constant, and T is the temperature. A general rule of thumb is that reactions with energy barrier of 0.9 eV (≈21 kcal/mol) or less from DFT calculations will proceed readily at room temperature.[60] The dissociation energy, E_{diss} determines whether the oxidation process is exothermic or endothermic. A negative value of E_{diss} implies the oxidation process to be exothermic, which is energetically favored. However, a positive value of E_{diss} indicates the oxidation process to be endothermic for which external sources are necessary to provide the required energy during this process. Thus, a large energy barrier combined with a positive value of the dissociation energy provides resistance to a 2D material toward oxidation, thereby improving the conditions for their applications in devices operating in air. In contrast, a material with low E_{barrier} (generally < 0.9 eV) and a negative value of E_{diss} is expected to be oxidized readily. The energy barrier and the dissociation energy can be obtained using DFT calculations by considering a series of possible oxidation pathways. The calculated E_{barrier} and E_{diss} for the considered 2D materials are listed in Table 1. These values will be used to explain the experiments in the following sections.

GROUP IV ELEMENTAL MONOLAYERS: GRAPHENE, SILICENE, AND GERMANENE

Graphene

Graphene remains one of the most extensively investigated 2D materials and has offered a wealth of information on the exotic physics and potential technological applications.[1–4,9,10,14,15,18–23,61] Graphene has a honeycomb structure with two carbon atoms in the unit cell. The carbon atoms are connected through σ bonds with sp^2 hybridized character. The out-of-plane p_z orbital forms the π bands which endows the observed linear dispersion near Fermi level.[62] Graphene can be synthesized by top–down strategy such as exfoliation from bulk graphite,[2,61] or bottom–up strategy such as chemical vapor deposition (CVD).[63–66] The readers can refer to a few comprehensive reviews on the fabrication, characterization, and application of graphene.[62,65,67–71]

Graphene shows extraordinary chemical stability in air at room temperature due to the robustness of the σ bonds and the out-of-plane π bonds. In fact, graphene has been used as a protection layer for metal substrates due to its excellent oxidation resistance.[72–76] As shown in Figure 2, graphene acts as a molecular diffusion barrier thus preventing the reactive agent from reaching the metal underneath.[72] Therefore, graphene coated Cu and Ni metals show very little visible change after annealing in air at

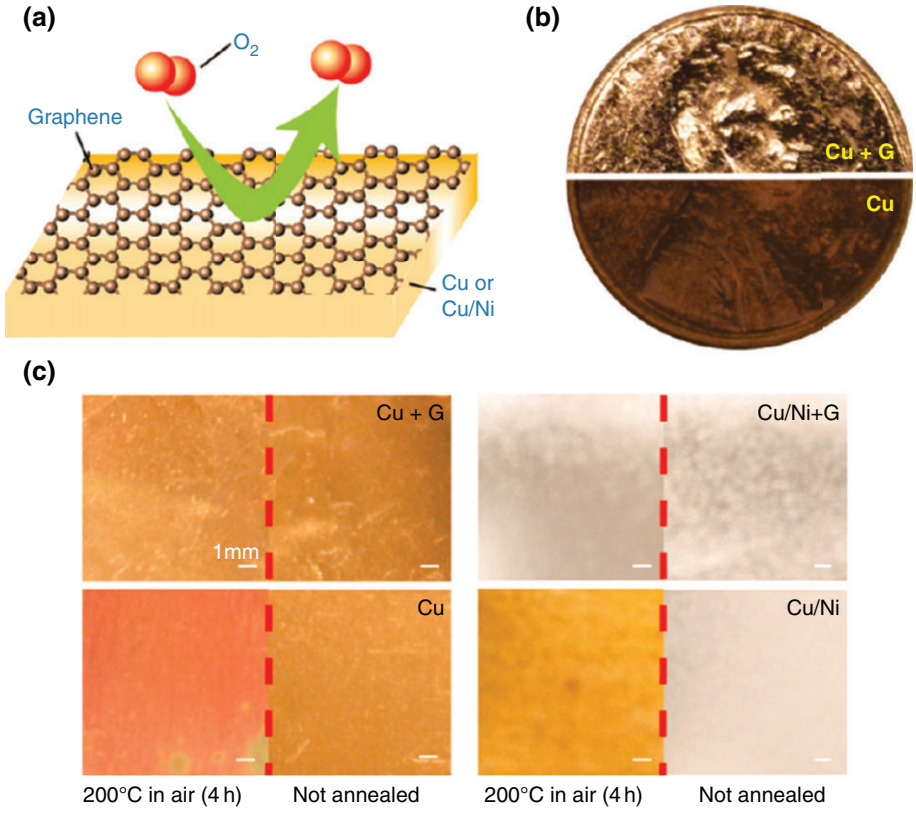

FIGURE 2 | Oxidation resistance of graphene coated Cu or Ni. (a) illustration of graphene as a chemically inert diffusion barrier, (b) photograph of graphene coated and uncoated penny after H_2O_2 treatment for 2 min, (c) photograph of Cu and Cu/Ni foil with and without graphene coating taken before and after annealing in air at 200°C for 4 h. (Reprinted with permission from Ref 72. Copyright 2011 American Chemical Society)

200°C for 4 h, while the surface of uncoated metal changes dramatically (Figures 2(c)).[72] Moreover, graphene can also provide short-term protection for metal exposed to an oxidizing aqueous solution of H_2O_2 (Figure 2(b)). While at temperature higher than 250°C, graphene starts to be reactive with O_2.[77] Li *et al.*[77] have shown oxidation induced strong hole doping in graphene at temperature from 200 to 300°C as revealed by Raman spectra, and the formation of etching pits at 500°C in O_2/Ar gas flow for 2 h as seen in Figure 3.[77,78]

Recent theoretical studies have begun to provide an insight into the oxidation resistance of graphene. As seen in Table 1, the oxidation barrier of the defect-free graphene is approximately 2.7 eV.[39] Moreover, the dissociation energy of O_2 molecule is 1.5 eV,[39] which implies the oxidation process to be endothermic. A large energy barrier and a positive value of the dissociation energy of O_2 molecule imply that the defect-free graphene has excellent oxidation resistance at room temperature. Therefore, instead of forming a chemical bond, O_2 prefers to physically adsorb to graphene surface at room temperature, which results in the reversible doping of graphene after treatment in a different environment.[79] However, at elevated temperatures, the thermal energy may overcome the energy barrier and trigger the irreversible oxidation of graphene. Both experiments and theory have shown that atomic O prefers to form epoxide group on graphene, i.e., an O atom covalently binds at the bridge site of two adjacent C atoms.[80–83] The epoxide groups have the preference to align in a line resulting in the fragmentation of graphene layer into smaller pieces upon oxidation.[84,85] It is interesting to note that the oxidized graphene fragments show rich spin structures, suggesting potential application in spintronic devices.[86]

Defects also play an important role in oxidation of graphene.[82] Defects are inevitable during the exfoliation or the growth process of 2D materials and have profound effects on their physical and chemical properties. Especially, the intrinsic defects, such as Stone–Wales (SW) defect, mono-vacancy, and di-vacancy with different configurations have been observed in graphene.[87–89] The calculated energy profiles of O_2 dissociation of on the defect-free and

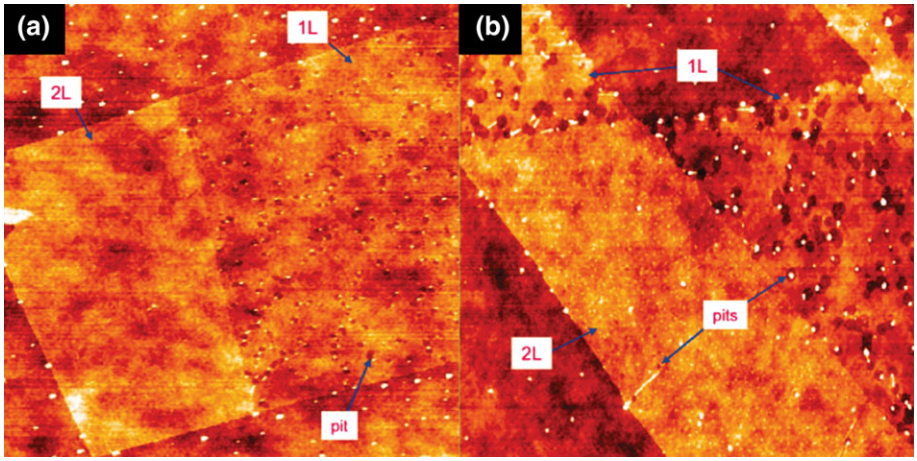

FIGURE 3 | Formation of pits in graphene. AFM images of oxidized single-layer (1L) and double-layer (2L) graphene: (a) oxidized at 500°C for 2 h with $P(O_2)$ = 350 torr, (b) oxidized at 600°C for 40 min with $P(O_2)$ = 260 torr. (Reprinted with permission from Ref 77. Copyright 2008 American Chemical Society)

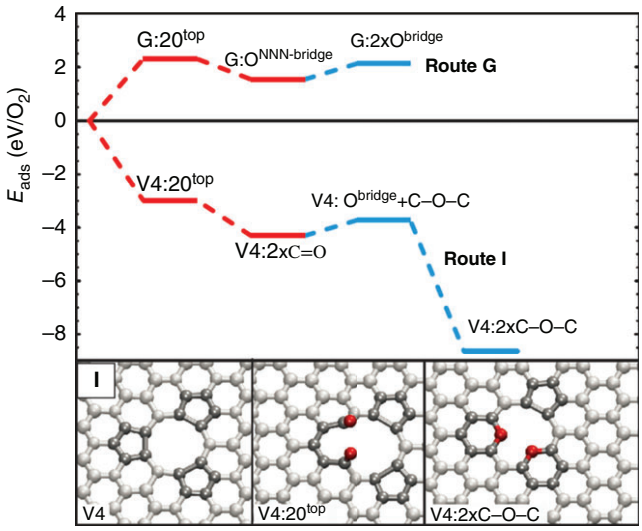

FIGURE 4 | Oxidation of graphene with and without defects. Upper panel: The adsorption energy for dissociative O_2 adsorption on perfect basal plane of graphene (route G) and at a bare four-atom vacancy (route I); Lower panel: The corresponding geometries of the stable mediate adsorption structures along route I. (Reprinted with permission from Ref 40. Copyright 2009 Creative Commons Attribution 3.0 License)

defective graphene is shown in Figure 4.[40] It can be seen that O_2 dissociation on the defect-free graphene is endothermic (Route G) with the bridge site to be the preferred adsorption site for O atom.[40] While O_2 dissociation on the defective graphene is highly exothermic with negligible barriers during the multistep process (Route I).[40] Therefore, O_2 could chemically adsorb on the defective graphene.[40,90,91] Based on the DFT calculation results, a two-step mechanism for oxidation of graphene has been proposed[40]: When exposed to O_2, (1) the bare vacancies in graphene are quickly saturated by ether and carbonyl groups and (2) the ether and carbonyl groups at the defect sites further activate the dissociation of O_2 leading to the formation of larger lactone groups, which could directly desorb CO or CO_2.[40,82] This two-step oxidation process leads to the etching of graphene with the formation of pits, as observed in recent experiments.[77,78,92,93]

Silicene

As the closest cousin of graphene belonging to the group IV elemental monolayers and being compatible with Si-based electronics, silicene has also attracted a great deal of attention from theorists and experimentalists.[94–96] The stronger spin orbit coupling in silicene compared to graphene makes it a potential candidate for the study of quantum spin Hall effect (QSHE).[97–99] The chemical bonds in silicene are different from those in the bulk: bulk Si is composed of sp^3 hybridized Si atoms; whereas silicene has a low buckled structure with mixed sp^2–sp^3 hybridized Si atoms.[100,101] Free-standing silicene is predicted to have linear dispersive band structure near Fermi level similar to that in graphene.[42,43] The buckled structure and sp^2–sp^3 hybridized bonds impart novel physical and chemical properties to silicene differentiating it from graphene.[102] Because of the nonexistence of a layered bulk counterpart, silicene cannot be isolated by exfoliation methods. Silicene has been grown by depositing Si atoms on Ag (111),[95,103–105] ZrB_2 (0001),[106] and MoS_2[107] substrates.

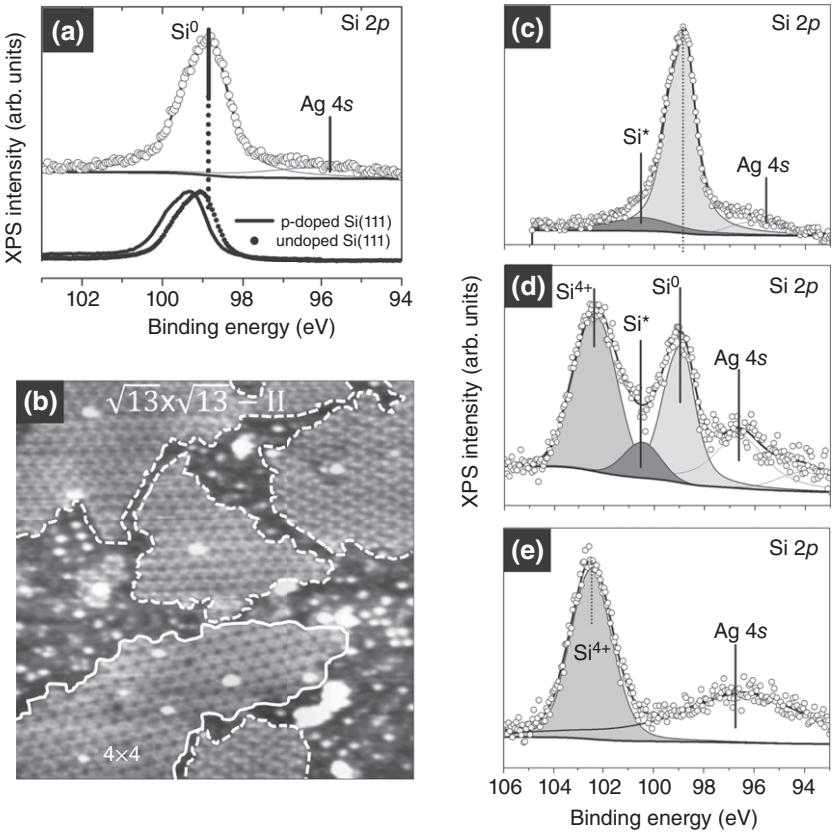

FIGURE 5 | Oxidation of silicene on Ag (111). (a) XPS line of silicene epitaxially grown on Ag (111), (b) STM topography of silicene with different domains, XPS of silicene exposed to 1000 L of O_2 (c), to air for 3 min (d), and to air for 1 day (e). (Reprinted with permission from Ref 31. Copyright 2013 Wiley-VCH Verlag GmbH & Co.)

Silicene is environmentally sensitive due to its mixed sp^2–sp^3 hybridization.[108] As revealed by X-ray Photoelectron Spectroscopy (XPS) measurements (Figure 5), the epitaxial silicene on Ag (111) substrate suffers from serious oxidation only after 3-min exposure to air (Figure 5(d)). After one day exposure to air, silicene film completely transforms to silica (Figure 5(e)).[31] The chemical instability of silicene in air limits its preparation to ultrahigh vacuum conditions and greatly hinders its applications in devices. Much efforts are needed on encapsulation at each step from material synthesis to fabrication of silicene-based devices. Recently, silicene-based field-effect transistor has been realized with *in situ* Al_2O_3 capping.[7] Padova *et al.*[109] have recently shown 24 h stability of thick multilayer silicene in air without passivation, which is due to the formation of an ultra-thin oxide on the surface preventing the rest of silicene from oxidation.

The oxidation energy barrier is calculated to be zero on silicene surface,[44] and the oxidation process is exothermic with the dissociation energy of O_2 molecule to be −4.0 to −5.4 eV.[44] Therefore, silicene is expected to spontaneously oxidize in O_2. Atomic O prefers to bind to the bridge site of two neighboring Si atoms in the 2D lattice.[44,110,111] The energy barrier for the O adatom moving on silicene is only 0.28 eV.[110] Therefore, atomic O could easily penetrate the surface leading to significant oxidation of silicene.[110] Interestingly, it is found that silicene shows low reactivity with pure O_2 when dosing up to 1000 L (Figure 5(c)).[31,112,113] The discrepancy between theory and experiments implies that other ingredients, such as the defects in silicene or humidity in the air or both potentially play critical roles in oxidation of silicene. However, at present, oxidation of silicene remains poorly understood and needs further studies.

Germanene

Germanene is another analogue of graphene belonging to group IV elemental monolayers. The structure of germanene is similar to that of silicene with a buckled lattice.[42] The Ge—Ge bonds in germanene show mixed sp^2–sp^3 hybridized character.[100] The

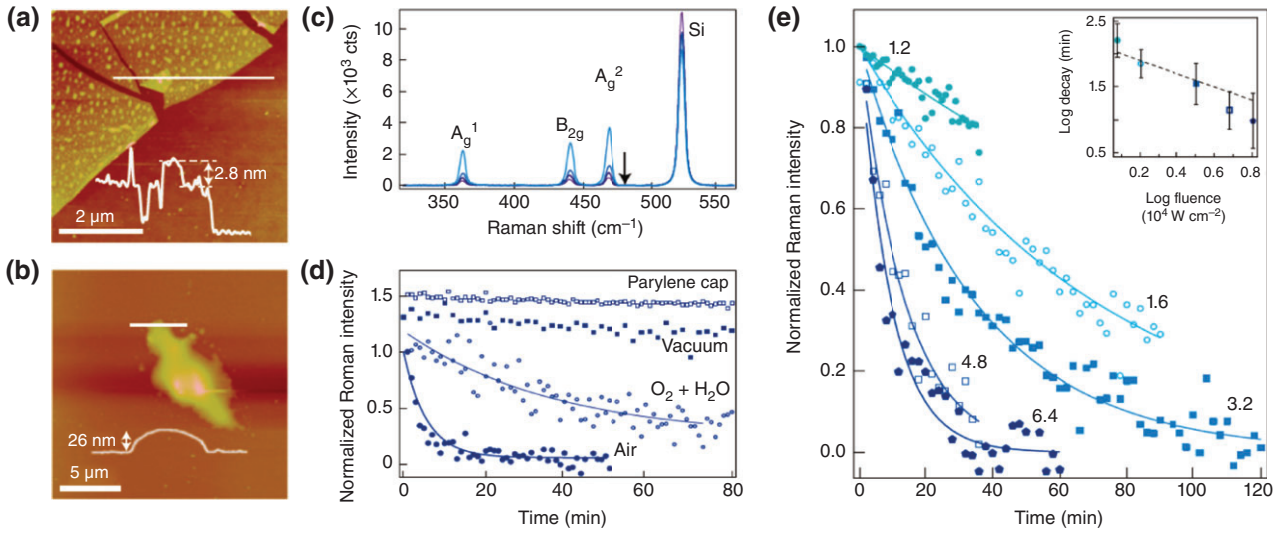

FIGURE 6 | Degradation of phosphorene. (a) AFM image of phosphorene after exfoliation, (b) after a few days under ambient conditions, (c) Raman spectra measured in air at 24, 48, 96, and 120 min after exfoliation, (d) time dependence of the integrated intensity of the A_g^2 mode in different conditions, (e) time evolution of the integrated A_g^2 mode at different laser fluences. (Reprinted with permission from Ref 57. Copyright 2015 Nature Publishing Group)

electronic properties of germanene have been extensively studied using DFT.[42,114–117] Atomically thin germanene has been recently synthesized on Au (111), Al (111), or Pt (111) surface,[118–120] while experimental reports on the interaction of germanene with O_2 are still lacking.

The oxidation energy barrier of germanene is calculated to be only 0.6 eV,[45,46] and the oxidation process is predicted to be exothermic with the dissociation energy of –2.3 to –2.5 eV.[45,46] The small cohesive energy of 3.4 to 4.2 eV[38,42] indicates the Ge—Ge bonds in germanene are much easier to break than C—C bonds in graphene. Therefore, germanene is also expected to be sensitive to O_2 at room temperature.

GROUP V ELEMENTAL MONOLAYER: PHOSPHORENE

Phosphorene is one of the recently rediscovered group V elemental monolayers.[6,121,122] A direct band gap, high carrier mobility, and anisotropic electronic and mechanical properties in phosphorene make it a promising candidate for applications in electronics and optoelectronics.[123,124] Different allotropes of phosphorene have been predicted.[125] The experimentally realized phosphorene, also sometimes referred to as black phosphorene, can be synthesized by mechanical[121,126] or liquid exfoliation[127,128] from its bulk counterpart, the black phosphorus, which is a layered material. In phosphorene, each P atom (with s^2p^3 valence electron configuration) shares three of its valence electrons with the neighboring P atoms, while the remaining valence electrons form a lone pair at the surface. Electron lone pairs on P atoms in phosphorene enhance its sensitivity to adatoms and a few adsorbed molecules.[129,130]

The exfoliated phosphorene samples quickly degrade in air.[32–34,57] As shown in Figure 6(a), bump-like structures form on the surface of the sample shortly after exposure to air.[57,130] These bumps grow in size and gradually deteriorate the sample after a few days.[57,130] Finally, the sample transforms to phosphoric acid, forming large droplets (Figure (b)).[57,130] Interestingly, the degradation of phosphorene is related to the presence of O_2, H_2O, and light. The degradation slows down when the sample is separately exposed to O_2, H_2O, and light (Figure 6(d) and (e)).[57]

Recent DFT calculations have addressed the origin of the degradation of phosphorene in air. The calculations predict the energy barrier of O_2 dissociation on phosphorene to be less than 0.5 eV[49] and the dissociation energy to be approximately –4.0 eV.[58] Therefore, phosphorene can easily oxidize with exposure to O_2. The atomic O prefers to bind to the dangling site on the surface by forming P═O bonds.[34,49,50,129] The oxidized species can further react with H_2O forming phosphoric acid.[58] The reaction of the oxidized species with H_2O results in the formation of extra extrinsic defects in phosphorene,[58] further promoting its photooxidation.[131] This oxidation process leads to the fast degradation of phosphorene in air. Other phosphorene allotropes, such as

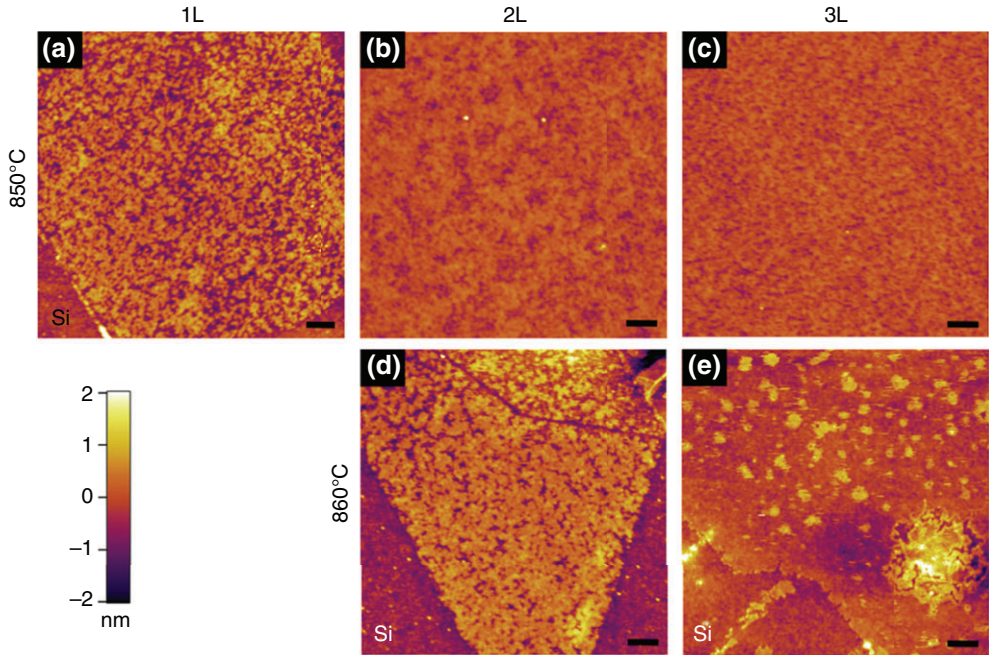

FIGURE 7 | AFM images of monolayer (1L), bilayer (2L), and trilayer (3L) *h*-BN after heating in air for 2 h. (Reprinted with permission from Ref 141. Copyright 2014 ACS AuthorChoice License)

blue phosphorene are also expected to be unstable in air.[58]

HEXAGONAL BORON NITRIDE

Hexagonal boron nitride (h-BN) monolayer, also known as 'white graphene,' is isoelectronic to graphene.[132,133] Both *h*-BN and graphene are comprised of sp^2 hybridized atoms with a planar honeycomb structure. The cohesive energy of *h*-BN is larger than 7.0 eV/atom,[51,52] which reflects the presence of strong in-plane bonds. However, unlike graphene, the electronegativity difference between B and N leads to a partial electron transfer from B to N, thereby giving an ionic bonding character to *h*-BN.[134] Moreover, unlike graphene, the *h*-BN sheets have a large band gap of approximately 6 eV, which allows them to be used as a dielectric in graphene based electronics. Multilayered *h*-BN have also been widely used in optoelectronics.[132] Large scale growth of *h*-BN has been achieved by CVD[135–137] as well as mechanical exfoliation.[138–140]

Multilayer *h*-BN is quite stable in air at room temperature. Li *et al.*[141] have recently demonstrated strong oxidation resistance of *h*-BN films. Although monolayer *h*-BN starts to oxidize at 700°C, it can sustain up to 850°C in air.[141] Annealing in air for 2 h at temperatures below 840°C does not cause dramatic changes in the surface morphology of *h*-BN films.[141] As seen in Figure 7(a), oxidative etching pits appear in *h*-BN monolayer after annealing in air at 850°C, and the monolayer burns out completely at 860°C.[141] Bilayer and trilayer *h*-BN can sustain even higher temperature than the monolayer (Figure 7(b)–(e)).[141] Thus, *h*-BN is suitable for high-temperature applications among the considered 2D materials. Strong oxidation resistance has also been reported for *h*-BN nanotubes, which are found to be stable in air up to 700°C.[142] Because of the excellent oxidation resistance, BN sheets have been utilized as coating layers to protect polymers from oxidative corrosion.[143]

DFT calculations have predicted the O_2 dissociation energy barrier on *h*-BN to be greater than 1.5 eV.[143] The O_2 dissociation process is endothermic with an energy increase of more than 1.2 eV.[143] The high energy barrier and the endothermic process indicate a strong oxidation resistance of *h*-BN, which is consistent with experimental observation.[141] The presence of point defects such as vacancies and SW defect are expected to reduce the oxidation resistance. Specifically, nitrogen vacancy has been predicted to reduce the oxidation energy barrier of *h*-BN nanotube to 0.8 eV,[144,145] and metal adatoms or substrates are expected to catalyze the dissociation of O_2 on *h*-BN.[146,147] Atomic O prefers to bind to the bridge site of B—N bond resulting in the elongation of the bond and a change in its nature from sp^2 to sp^3 hybridization.[53] The adsorbed O atoms tend to

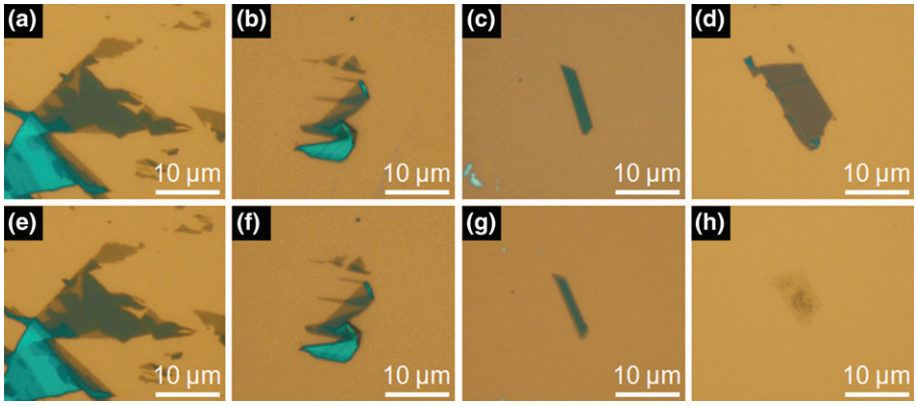

FIGURE 8 | Optical images of mechanically exfoliated MoS_2 nanosheets before (a–d) and after (e–h) thermal annealing in air for 1 h at 260°C (e), 300°C (f), 330°C (g), and 400°C (h). (Reprinted with permission from Ref 168. Copyright 2013 Wiley-VCH Verlag GmbH & Co.)

form energy-favorable domains or chains leading to the formation of elongated etching pits and fracture on *h*-BN,[53,148] which explains the experimental results.[141]

MOLYBDENUM DISULFIDE

Transition metal dichalcogenides (TMDCs) are a large family of layered materials with unique electronic and optical properties.[149] Bulk TMDCs are stacked together by a weak van der Waals (vdW) interaction which allows the exfoliation of the material down to monolayer.[149–151] The properties of TMDCs depend on the structure and the stoichiometry leading to rich physics and chemistry in these materials.[152,153] MoS_2 is a representative and most investigated member in the TMDCs family. Bulk MoS_2 is a semiconductor with an indirect band gap of 1.2 eV.[154] The monolayer has a direct band gap of 1.8 eV, which makes it a promising candidate for next generation high-speed field-effect transistors (FETs) and optoelectronic devices.[5,155–157] In monolayer MoS_2, the Mo atoms are sandwiched between two layers of S atoms. Each Mo atom is surrounded by six neighboring S atoms. The p orbitals of S atoms hybridize with the d orbitals of Mo atoms, forming p–d hybridized ionic Mo—S bonds.[158,159] Several experimental methods including mechanical exfoliation,[5,8,152,160,161] CVD and metal–organic (MO) CVD[66,162–165] have been used to fabricate MoS_2 monolayers.

MoS_2 shows good stability in air at room temperature. A few experiments and theoretical calculations have demonstrated that MoS_2 could be used as a passivation or protection layer to prevent oxidation of other materials.[166,167] Oxidation of MoS_2 occurs at temperature higher than 300°C in air. Wu *et al.*[168] have reported significant thinning and etching of MoS_2 after 1 h annealing at temperature higher than 330°C in air (Figure 8(c), (d), (g), and (h)); At temperatures below 330°C, annealing in air does not cause significant change in its morphology (Figure 8 (a), (b), (e), and (f)). The thinning and etching processes occur due to oxidation of MoS_2, forming a transparent layer of MoO_3.[168,169] Long-time thermal annealing in Ar/O_2 mixture at temperatures higher than 320°C introduces oxidative etching pits in MoS_2, which have been utilized to pattern MoS_2 sheets with well-oriented etching pits.[168,170–172] Yamamoto *et al.*[172] have shown that the edges of the triangular etching pits have the preference along zigzag direction as shown in Figure 9, and the etching is initiated at the native defect sites and grows laterally on the surface of MoS_2.[172]

The calculated oxidation energy barrier on MoS_2 is 1.6 eV.[56] The large energy barrier explains the good stability of MoS_2 against oxidation at room temperature. Similar to graphene and *h*-BN, presence of atomic-level defects significantly alter the mechanism of O_2 adsorption in MoS_2.[56] Sulfur vacancies at the surface of MoS_2 is expected to reduce the oxidation energy barrier to 0.8 eV.[56] Therefore, defect sites on MoS_2 surface exhibit high reactivity and are readily filled by oxygen atoms.[56] These defective sites are also expected to act as the seeds that initiate the etching of MoS_2. The theoretical calculation agrees very well with the experiment observation of the etching of MoS_2 starting at the native defect sites in the 2D lattice.[172]

CONCLUSION AND OUTLOOK

In summary, we have presented a review of the recent experiments and theoretical studies addressing oxidation of selected 2D nanomaterials by molecular

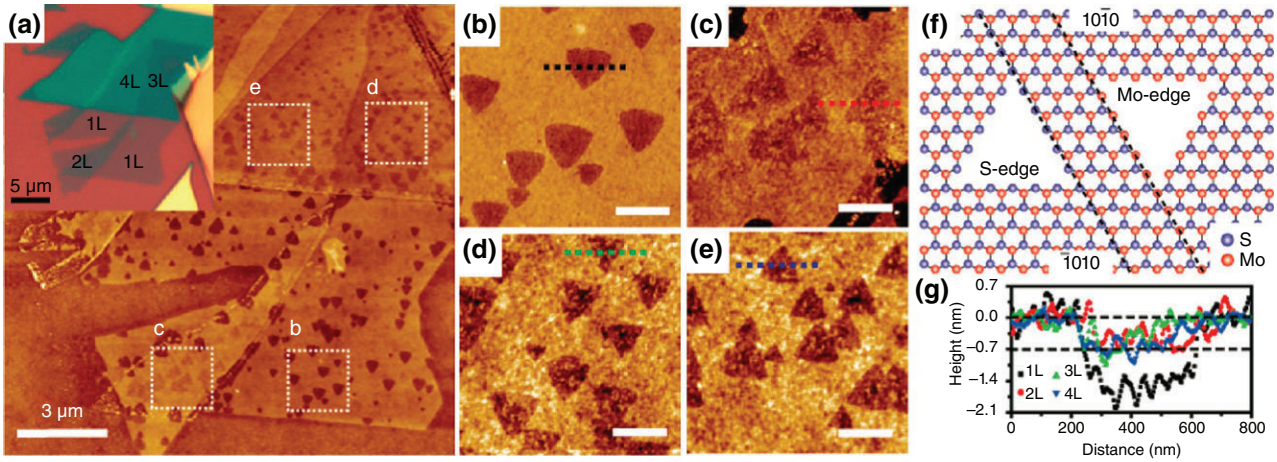

FIGURE 9 | Oxidation of MoS_2. (a) AFM images of MoS_2 annealing in Ar/O_2 mixture at 320°C for 3 h, (b–e) close-up images of the areas surrounded by dashed lines in the panel (a), (f) schematic drawing of MoS_2 with triangular pits, (g) profiles of pits along the dashed lines in (b–e). (Reprinted with permission from Ref 172. Copyright 2013 American Chemical Society)

O_2. Depending on their structures and chemistries, oxidation of 2D nanomaterials has a wide variation. The combination of experiments and calculations reveals a significant role of the structure, chemical bonds and native defects in 2D materials for their practical applications in devices. With the advances in the exfoliation and synthesis techniques, several new atomically thin materials have emerged and the family of 2D materials continues to grow. Novel 2D materials hold great promise for future applications. But challenges remain in scaled up, high purity synthesis/growth, characterization, and integration of these materials into devices. Effective passivation or encapsulation methods need to be developed for 2D materials, such as silicene, germanene, and phosphorene, which are very promising for high-speed electronics, optoelectronics, and sensor applications, but found to be chemically unstable in the presence of oxygen. We hope this review encourages further investigations of the environmental effects on the structure and properties of 2D materials.

ACKNOWLEDGMENTS

This research was partially supported by a Cooperative Research Agreement (# W911NF-14-2-0088) with the Army Research Laboratory through Army Research Office. We thank Dr. J. Zabinski for his interest and helpful advice on this work.

REFERENCES

1. Novoselov KS, Geim AK, Morozov S, Jiang D, Zhang Y, Sa D, Grigorieva I, Firsov A. Electric field effect in atomically thin carbon films. *Science* 2004, 306:666–669.
2. Geim AK, Novoselov KS. The rise of graphene. *Nat Mater* 2007, 6:183–191.
3. Schwierz F. Graphene transistors. *Nat Nanotechnol* 2010, 5:487–496.
4. Britnell L, Gorbachev R, Jalil R, Belle B, Schedin F, Mishchenko A, Georgiou T, Katsnelson M, Eaves L, Morozov S. Field-effect tunneling transistor based on vertical graphene heterostructures. *Science* 2012, 335:947–950.
5. Radisavljevic B, Radenovic A, Brivio J, Giacometti V, Kis A. Single-layer MoS_2 transistors. *Nat Nanotechnol* 2011, 6:147–150.
6. Li L, Yu Y, Ye GJ, Ge Q, Ou X, Wu H, Feng D, Chen XH, Zhang Y. Black phosphorus field-effect transistors. *Nat Nanotechnol* 2014, 9:372–377.
7. Tao L, Cinquanta E, Chiappe D, Grazianetti C, Fanciulli M, Dubey M, Molle A, Akinwande D. Silicene field-effect transistors operating at room temperature. *Nat Nanotechnol* 2015, 10:227–231.
8. Yin Z, Li H, Li H, Jiang L, Shi Y, Sun Y, Lu G, Zhang Q, Chen X, Zhang H. Single-layer MoS_2 phototransistors. *ACS Nano* 2011, 6:74–80.

9. Dan Y, Lu Y, Kybert NJ, Luo Z, Johnson AC. Intrinsic response of graphene vapor sensors. *Nano Lett* 2009, 9:1472–1475.
10. Dua V, Surwade SP, Ammu S, Agnihotra SR, Jain S, Roberts KE, Park S, Ruoff RS, Manohar SK. All-organic vapor sensor using inkjet-printed reduced graphene oxide. *Angew Chem Int Ed* 2010, 49:2154–2157.
11. Perkins FK, Friedman AL, Cobas E, Campbell P, Jernigan G, Jonker BT. Chemical vapor sensing with monolayer MoS_2. *Nano Lett* 2013, 13:668–673.
12. Late DJ, Huang Y-K, Liu B, Acharya J, Shirodkar SN, Luo J, Yan A, Charles D, Waghmare UV, Dravid VP. Sensing behavior of atomically thin-layered MoS_2 transistors. *ACS Nano* 2013, 7:4879–4891.
13. Abbas AN, Liu B, Chen L, Ma Y, Cong S, Aroonyadet N, Köpf M, Nilges T, Zhou C. Black phosphorus gas sensors. *ACS Nano* 2015, 9:5618–5624.
14. Stoller MD, Park S, Zhu Y, An J, Ruoff RS. Graphene-based ultracapacitors. *Nano Lett* 2008, 8:3498–3502.
15. Yoo E, Kim J, Hosono E, H-s Z, Kudo T, Honma I. Large reversible Li storage of graphene nanosheet families for use in rechargeable lithium ion batteries. *Nano Lett* 2008, 8:2277–2282.
16. Wang D, Choi D, Li J, Yang Z, Nie Z, Kou R, Hu D, Wang C, Saraf LV, Zhang J. Self-assembled TiO_2–graphene hybrid nanostructures for enhanced Li-ion insertion. *ACS Nano* 2009, 3:907–914.
17. Hwang H, Kim H, Cho J. MoS_2 nanoplates consisting of disordered graphene-like layers for high rate lithium battery anode materials. *Nano Lett* 2011, 11:4826–4830.
18. Wu J, Becerril HA, Bao Z, Liu Z, Chen Y, Peumans P. Organic solar cells with solution-processed graphene transparent electrodes. *Appl Phys Lett* 2008, 92:263302.
19. Wang X, Zhi L, Müllen K. Transparent, conductive graphene electrodes for dye-sensitized solar cells. *Nano Lett* 2008, 8:323–327.
20. Miao X, Tongay S, Petterson MK, Berke K, Rinzler AG, Appleton BR, Hebard AF. High efficiency graphene solar cells by chemical doping. *Nano Lett* 2012, 12:2745–2750.
21. Han T-H, Lee Y, Choi M-R, Woo S-H, Bae S-H, Hong BH, Ahn J-H, Lee T-W. Extremely efficient flexible organic light-emitting diodes with modified graphene anode. *Nat Photonics* 2012, 6:105–110.
22. Wu J, Agrawal M, Becerril HA, Bao Z, Liu Z, Chen Y, Peumans P. Organic light-emitting diodes on solution-processed graphene transparent electrodes. *ACS Nano* 2009, 4:43–48.
23. Bonaccorso F, Sun Z, Hasan T, Ferrari A. Graphene photonics and optoelectronics. *Nat Photonics* 2010, 4:611–622.
24. Splendiani A, Sun L, Zhang Y, Li T, Kim J, Chim C-Y, Galli G, Wang F. Emerging photoluminescence in monolayer MoS_2. *Nano Lett* 2010, 10:1271–1275.
25. Eda G, Yamaguchi H, Voiry D, Fujita T, Chen M, Chhowalla M. Photoluminescence from chemically exfoliated MoS_2. *Nano Lett* 2011, 11:5111–5116.
26. Ross JS, Klement P, Jones AM, Ghimire NJ, Yan J, Mandrus D, Taniguchi T, Watanabe K, Kitamura K, Yao W. Electrically tunable excitonic light-emitting diodes based on monolayer WSe_2 pn junctions. *Nat Nanotechnol* 2014, 9:268–272.
27. Salehzadeh O, Tran NH, Liu X, Shih I, Mi Z. Exciton kinetics, quantum efficiency, and efficiency droop of monolayer mos_2 light-emitting devices. *Nano Lett* 2014, 14:4125–4130.
28. Dreyer DR, Park S, Bielawski CW, Ruoff RS. The chemistry of graphene oxide. *Chem Soc Rev* 2010, 39:228–240.
29. Eda G, Fanchini G, Chhowalla M. Large-area ultrathin films of reduced graphene oxide as a transparent and flexible electronic material. *Nat Nanotechnol* 2008, 3:270–274.
30. Stankovich S, Dikin DA, Piner RD, Kohlhaas KA, Kleinhammes A, Jia Y, Wu Y, Nguyen ST, Ruoff RS. Synthesis of graphene-based nanosheets via chemical reduction of exfoliated graphite oxide. *Carbon* 2007, 45:1558–1565.
31. Molle A, Grazianetti C, Chiappe D, Cinquanta E, Cianci E, Tallarida G, Fanciulli M. Hindering the oxidation of silicene with non-reactive encapsulation. *Adv Funct Mater* 2013, 23:4340–4344.
32. Andres C-G, Leonardo V, Elsa P, Joshua OI, Narasimha-Acharya KL, Sofya IB, Dirk JG, Michele B, Gary AS, Alvarez JV, et al. Isolation and characterization of few-layer black phosphorus. *2D Mater* 2014, 1:025001.
33. Island JO, Steele GA, van der Zant HS, Castellanos-Gomez A. Environmental instability of few-layer black phosphorus. *2D Mater* 2015, 2:011002.
34. Wood JD, Wells SA, Jariwala D, Chen K-S, Cho E, Sangwan VK, Liu X, Lauhon LJ, Marks TJ, Hersam MC. Effective passivation of exfoliated black phosphorus transistors against ambient degradation. *Nano Lett* 2014, 14:6964–6970.
35. Dreizler RM, Gross EK. *Density Functional Theory: An Approach to the Quantum Many-Body Problem*. Berlin Heidelberg: Springer-Verlag; 2012.
36. Koskinen P, Malola S, Häkkinen H. Self-passivating edge reconstructions of graphene. *Phys Rev Lett* 2008, 101:115502.

37. Barone V, Hod O, Scuseria GE. Electronic structure and stability of semiconducting graphene nanoribbons. *Nano Lett* 2006, 6:2748–2754.
38. Matusalem F, Marques M, Teles LK, Bechstedt F. Stability and electronic structure of two-dimensional allotropes of group-IV materials. *Phys Rev B* 2015, 92:045436.
39. Ni S, Li Z, Yang J. Oxygen molecule dissociation on carbon nanostructures with different types of nitrogen doping. *Nanoscale* 2012, 4:1184–1189.
40. Carlsson JM, Hanke F, Linic S, Scheffler M. Two-step mechanism for low-temperature oxidation of vacancies in graphene. *Phys Rev Lett* 2009, 102:166104.
41. Bian G, Wang X, Liu Y, Miller T, Chiang TC. Interfacial protection of topological surface states in ultrathin Sb films. *Phys Rev Lett* 2012, 108:176401.
42. Cahangirov S, Topsakal M, Aktürk E, Şahin H, Ciraci S. Two- and one-dimensional honeycomb structures of silicon and germanium. *Phys Rev Lett* 2009, 102:236804.
43. Drummond ND, Zólyomi V, Fal'ko VI. Electrically tunable band gap in silicene. *Phys Rev B* 2012, 85:075423.
44. Liu G, Lei XL, Wu MS, Xu B, Ouyang CY. Is silicene stable in O_2?—first-principles study of O_2 dissociation and O_2-dissociation-induced oxygen atoms adsorption on free-standing silicene. *Europhys Lett* 2014, 106:47001.
45. Liu G, Liu SB, Xu B, Ouyang CY, Song HY. First-principles study of the stability of free-standing germanene in oxygen atmosphere. *J Appl Phys* 2015, 118:124303.
46. Xia W, Hu W, Li Z, Yang J. A first-principles study of gas adsorption on germanene. *Phys Chem Chem Phys* 2014, 16:22495–22498.
47. Guan J, Zhu Z, Tománek D. Phase coexistence and metal-insulator transition in few-layer phosphorene: a computational study. *Phys Rev Lett* 2014, 113:046804.
48. Cai Y, Zhang G, Zhang Y-W. Layer-dependent band alignment and work function of few-layer phosphorene. *Sci Rep* 2014, 4:6677.
49. Ziletti A, Carvalho A, Campbell D, Coker D, Neto AC. Oxygen defects in phosphorene. *Phys Rev Lett* 2015, 114:046801.
50. Wang G, Pandey R, Karna SP. Phosphorene oxide: stability and electronic properties of a novel two-dimensional material. *Nanoscale* 2015, 7:524–531.
51. Ooi N, Rajan V, Gottlieb J, Catherine Y, Adams JB. Structural properties of hexagonal boron nitride. *Model Simul Mater Sci Eng* 2006, 14:515.
52. Yin L-C, Cheng H-M, Saito R. Triangle defect states of hexagonal boron nitride atomic layer: density functional theory calculations. *Phys Rev B* 2010, 81:153407.
53. Zhao Y, Wu X, Yang J, Zeng XC. Oxidation of a two-dimensional hexagonal boron nitride monolayer: a first-principles study. *Phys Chem Chem Phys* 2012, 14:5545–5550.
54. Ahmad S, Mukherjee S. A comparative study of electronic properties of bulk MoS_2 and its monolayer using DFT technique: application of mechanical strain on MoS_2 monolayer. *Graphene* 2014, 3:52.
55. Ataca C, Topsakal M, Aktürk E, Ciraci S. A comparative study of lattice dynamics of three- and two-dimensional MoS_2. *J Phys Chem C* 2011, 115:16354–16361.
56. Santosh K, Longo RC, Wallace RM, Cho K. Surface oxidation energetics and kinetics on MoS_2 monolayer. *J Appl Phys* 2015, 117:135301.
57. Favron A, Gaufres E, Fossard F, Phaneuf-Lheureux A-L, Tang NYW, Levesque PL, Loiseau A, Leonelli R, Francoeur S, Martel R. Photooxidation and quantum confinement effects in exfoliated black phosphorus. *Nat Mater* 2015, 14:826–832.
58. Gaoxue W, William JS, Ravindra P, Shashi PK. Degradation of phosphorene in air: understanding at atomic level. *2D Mater* 2016, 3:025011.
59. Arrhenius S. Über die reaktionsgeschwindigkeit bei der inversion von rohrzucker durch säuren. *Z Phys Chem* 1889, 4:226–248.
60. Young D. *Computational Chemistry: A Practical Guide for Applying Techniques to Real World Problems*. New York: John Wiley & Sons; 2004.
61. Novoselov K, Geim AK, Morozov S, Jiang D, Grigorieva MKI, Dubonos S, Firsov A. Two-dimensional gas of massless Dirac fermions in graphene. *Nature* 2005, 438:197–200.
62. Neto AC, Guinea F, Peres N, Novoselov KS, Geim AK. The electronic properties of graphene. *Rev Mod Phys* 2009, 81:109.
63. Yu Q, Lian J, Siriponglert S, Li H, Chen YP, Pei S-S. Graphene segregated on Ni surfaces and transferred to insulators. *Appl Phys Lett* 2008, 93:113103.
64. Reina A, Jia X, Ho J, Nezich D, Son H, Bulovic V, Dresselhaus MS, Kong J. Large area, few-layer graphene films on arbitrary substrates by chemical vapor deposition. *Nano Lett* 2008, 9:30–35.
65. Zhang Y, Zhang L, Zhou C. Review of chemical vapor deposition of graphene and related applications. *Acc Chem Res* 2013, 46:2329–2339.
66. Kang K, Xie S, Huang L, Han Y, Huang PY, Mak KF, Kim C-J, Muller D, Park J. High-mobility three-atom-thick semiconducting films with wafer-scale homogeneity. *Nature* 2015, 520:656–660.
67. Choi W, Lahiri I, Seelaboyina R, Kang YS. Synthesis of graphene and its applications: a review. *Crit Rev Solid State Mater Sci* 2010, 35:52–71.
68. Allen MJ, Tung VC, Kaner RB. Honeycomb carbon: a review of graphene. *Chem Rev* 2009, 110:132–145.

69. Wang H, Maiyalagan T, Wang X. Review on recent progress in nitrogen-doped graphene: synthesis, characterization, and its potential applications. *ACS Catal* 2012, 2:781–794.

70. Shao Y, Wang J, Wu H, Liu J, Aksay IA, Lin Y. Graphene based electrochemical sensors and biosensors: a review. *Electroanalysis* 2010, 22:1027–1036.

71. Mattevi C, Kim H, Chhowalla M. A review of chemical vapour deposition of graphene on copper. *J Mater Chem* 2011, 21:3324–3334.

72. Chen S, Brown L, Levendorf M, Cai W, Ju S-Y, Edgeworth J, Li X, Magnuson CW, Velamakanni A, Piner RD. Oxidation resistance of graphene-coated Cu and Cu/Ni alloy. *ACS Nano* 2011, 5:1321–1327.

73. Kang D, Kwon JY, Cho H, Sim J-H, Hwang HS, Kim CS, Kim YJ, Ruoff RS, Shin HS. Oxidation resistance of iron and copper foils coated with reduced graphene oxide multilayers. *ACS Nano* 2012, 6:7763–7769.

74. Gadipelli S, Calizo I, Ford J, Cheng G, Walker ARH, Yildirim T. A highly practical route for large-area, single layer graphene from liquid carbon sources such as benzene and methanol. *J Mater Chem* 2011, 21:16057–16065.

75. Topsakal M, Şahin H, Ciraci S. Graphene coatings: an efficient protection from oxidation. *Phys Rev B* 2012, 85:155445.

76. Cho J, Gao L, Tian J, Cao H, Wu W, Yu Q, Yitamben EN, Fisher B, Guest JR, Chen YP, et al. Atomic-scale investigation of graphene grown on Cu foil and the effects of thermal annealing. *ACS Nano* 2011, 5:3607–3613.

77. Liu L, Ryu S, Tomasik MR, Stolyarova E, Jung N, Hybertsen MS, Steigerwald ML, Brus LE, Flynn GW. Graphene oxidation: thickness-dependent etching and strong chemical doping. *Nano Lett* 2008, 8:1965–1970.

78. Jones J, Morris C, Verbeck G, Perez J. Oxidative pit formation in pristine, hydrogenated and dehydrogenated graphene. *Appl Surf Sci* 2013, 264:853–863.

79. Ryu S, Liu L, Berciaud S, Yu Y-J, Liu H, Kim P, Flynn GW, Brus LE. Atmospheric oxygen binding and hole doping in deformed graphene on a SiO_2 substrate. *Nano Lett* 2010, 10:4944–4951.

80. Vinogradov N, Schulte K, Ng ML, Mikkelsen A, Lundgren E, Martensson N, Preobrajenski A. Impact of atomic oxygen on the structure of graphene formed on Ir (111) and Pt (111). *J Phys Chem C* 2011, 115:9568–9577.

81. Yan J-A, Chou M. Oxidation functional groups on graphene: structural and electronic properties. *Phys Rev B* 2010, 82:125403.

82. Barinov A, Malcioglu OB, Fabris S, Sun T, Gregoratti L, Dalmiglio M, Kiskinova M. Initial stages of oxidation on graphitic surfaces: photoemission study and density functional theory calculations. *J Phys Chem C* 2009, 113:9009–9013.

83. Šljivančanin Ž, Milošević AS, Popović ZS, Vukajlović FR. Binding of atomic oxygen on graphene from small epoxy clusters to a fully oxidized surface. *Carbon* 2013, 54:482–488.

84. Li Z, Zhang W, Luo Y, Yang J, Hou JG. How graphene is cut upon oxidation? *J Am Chem Soc* 2009, 131:6320–6321.

85. Li J-L, Kudin KN, McAllister MJ, Prud'homme RK, Aksay IA, Car R. Oxygen-driven unzipping of graphitic materials. *Phys Rev Lett* 2006, 96:176101.

86. Gao X, Wang L, Ohtsuka Y, D-e J, Zhao Y, Nagase S, Chen Z. Oxidation unzipping of stable nanographenes into joint spin-rich fragments. *J Am Chem Soc* 2009, 131:9663–9669.

87. Ugeda MM, Brihuega I, Hiebel F, Mallet P, Veuillen J-Y, Gómez-Rodríguez JM, Ynduráin F. Electronic and structural characterization of divacancies in irradiated graphene. *Phys Rev B* 2012, 85:121402.

88. Hashimoto A, Suenaga K, Gloter A, Urita K, Iijima S. Direct evidence for atomic defects in graphene layers. *Nature* 2004, 430:870–873.

89. Banhart F, Kotakoski J, Krasheninnikov AV. Structural defects in graphene. *ACS Nano* 2011, 5:26–41.

90. Sun T, Fabris S, Baroni S. Surface precursors and reaction mechanisms for the thermal reduction of graphene basal surfaces oxidized by atomic oxygen. *J Phys Chem C* 2011, 115:4730–4737.

91. Qi X, Guo X, Zheng C. Density functional study the interaction of oxygen molecule with defect sites of graphene. *Appl Surf Sci* 2012, 259:195–200.

92. Yamada Y, Murota K, Fujita R, Kim J, Watanabe A, Nakamura M, Sato S, Hata K, Ercius P, Ciston J, et al. Subnanometer vacancy defects introduced on graphene by oxygen gas. *J Am Chem Soc* 2014, 136:2232–2235.

93. Lee SM, Lee YH, Hwang YG, Hahn J, Kang H. Defect-induced oxidation of graphite. *Phys Rev Lett* 1999, 82:217.

94. Kara A, Enriquez H, Seitsonen AP, Lew Yan Voon LC, Vizzini S, Aufray B, Oughaddou H. A review on silicene—new candidate for electronics. *Surf Sci Rep* 2012, 67:1–18.

95. Vogt P, De Padova P, Quaresima C, Avila J, Frantzeskakis E, Asensio MC, Resta A, Ealet B, Le Lay G. Silicene: compelling experimental evidence for graphenelike two-dimensional silicon. *Phys Rev Lett* 2012, 108:155501.

96. Lalmi B, Oughaddou H, Enriquez H, Kara A, Vizzini S, Ealet B, Aufray B. Epitaxial growth of a silicene sheet. *Appl Phys Lett* 2010, 97:223109.

97. Liu C-C, Feng W, Yao Y. Quantum spin Hall effect in silicene and two-dimensional germanium. *Phys Rev Lett* 2011, 107:076802.

98. Ezawa M. Valley-polarized metals and quantum anomalous Hall effect in silicene. *Phys Rev Lett* 2012, 109:055502.

99. Ezawa M. A topological insulator and helical zero mode in silicene under an inhomogeneous electric field. *New J Phys* 2012, 14:033003.

100. Takeda K, Shiraishi K. Theoretical possibility of stage corrugation in Si and Ge analogs of graphite. *Phys Rev B* 1994, 50:14916–14922.

101. Yukiko Y-T, Rainer F. Progress in the materials science of silicene. *Sci Technol Adv Mater* 2014, 15:064404.

102. Jose D, Datta A. Structures and chemical properties of silicene: unlike graphene. *Acc Chem Res* 2014, 47:593–602.

103. Lin C-L, Arafune R, Kawahara K, Tsukahara N, Minamitani E, Kim Y, Takagi N, Kawai M. Structure of silicene grown on Ag (111). *Appl Phys Exp* 2012, 5:045802.

104. Jamgotchian H, Colignon Y, Hamzaoui N, Ealet B, Hoarau J, Aufray B, Bibérian J. Growth of silicene layers on Ag (111): unexpected effect of the substrate temperature. *J Phys Condens Matter* 2012, 24:172001.

105. Feng B, Ding Z, Meng S, Yao Y, He X, Cheng P, Chen L, Wu K. Evidence of silicene in honeycomb structures of silicon on Ag (111). *Nano Lett* 2012, 12:3507–3511.

106. Fleurence A, Friedlein R, Ozaki T, Kawai H, Wang Y, Yamada-Takamura Y. Experimental evidence for epitaxial silicene on diboride thin films. *Phys Rev Lett* 2012, 108:245501.

107. Chiappe D, Scalise E, Cinquanta E, Grazianetti C, van den Broek B, Fanciulli M, Houssa M, Molle A. Two-dimensional Si nanosheets with local hexagonal structure on a MoS_2 surface. *Adv Mater* 2014, 26:2096–2101.

108. Cinquanta E, Scalise E, Chiappe D, Grazianetti C, van den Broek B, Houssa M, Fanciulli M, Molle A. Getting through the nature of silicene: an sp^2–sp^3 two-dimensional silicon nanosheet. *J Phys Chem C* 2013, 117:16719–16724.

109. De Padova P, Ottaviani C, Quaresima C, Olivieri B, Imperatori P, Salomon E, Angot T, Quagliano L, Romano C, Vona A. 24 h stability of thick multilayer silicene in air. *2D Mater* 2014, 1:1003.

110. Özçelik VO, Ciraci S. Local reconstructions of silicene induced by adatoms. *J Phys Chem C* 2013, 117:26305–26315.

111. Xu X, Zhuang J, Du Y, Feng H, Zhang N, Liu C, Lei T, Wang J, Spencer M, Morishita T. Effects of oxygen adsorption on the surface state of epitaxial silicene on Ag (111). *Sci Rep* 2014, 4:7543.

112. Friedlein R, Van Bui H, Wiggers F, Yamada-Takamura Y, Kovalgin A, de Jong M. Interaction of epitaxial silicene with overlayers formed by exposure to Al atoms and O_2 molecules. *J Chem Phys* 2014, 140:204705.

113. De Padova P, Quaresima C, Olivieri B, Perfetti P, Le Lay G. Strong resistance of silicene nanoribbons towards oxidation. *J Phys D Appl Phys* 2011, 44:312001.

114. Nijamudheen A, Bhattacharjee R, Choudhury S, Datta A. Electronic and chemical properties of germanene: the crucial role of buckling. *J Phys Chem C* 2015, 119:3802–3809.

115. Ni Z, Liu Q, Tang K, Zheng J, Zhou J, Qin R, Gao Z, Yu D, Lu J. Tunable bandgap in silicene and germanene. *Nano Lett* 2011, 12:113–118.

116. Bechstedt F, Matthes L, Gori P, Pulci O. Infrared absorbance of silicene and germanene. *Appl Phys Lett* 2012, 100:261906.

117. Roome NJ, Carey JD. Beyond graphene: stable elemental monolayers of silicene and germanene. *ACS Appl Mater Interfaces* 2014, 6:7743–7750.

118. Dávila ME, Xian L, Cahangirov S, Rubio A, Lay GL. Germanene: a novel two-dimensional germanium allotrope akin to graphene and silicene. *New J Phys* 2014, 16:095002.

119. Derivaz M, Dentel D, Stephan R, Hanf M-C, Mehdaoui A, Sonnet P, Pirri C. Continuous germanene layer on Al (111). *Nano Lett* 2015, 15:2510–2516.

120. Li L, Lu S, Pan J, Qin Z, Wang Y, Wang Y, Cao Gy DS, Gao HJ. Buckled germanene formation on Pt (111). *Adv Mater* 2014, 26:4820–4824.

121. Liu H, Neal AT, Zhu Z, Luo Z, Xu X, Tománek D, Ye PD. Phosphorene: an unexplored 2D semiconductor with a high hole mobility. *ACS Nano* 2014, 8:4033–4041.

122. Wang G, Pandey R, Karna SP. Atomically thin group V elemental films: theoretical investigations of antimonene allotropes. *ACS Appl Mater Interfaces* 2015, 7:11490–11496.

123. Xia F, Wang H, Jia Y. Rediscovering black phosphorus as an anisotropic layered material for optoelectronics and electronics. *Nat Commun* 2014, 5:4458.

124. Fei R, Yang L. Strain-engineering the anisotropic electrical conductance of few-layer black phosphorus. *Nano Lett* 2014, 14:2884–2889.

125. Zhu Z, Tománek D. Semiconducting layered blue phosphorus: a computational study. *Phys Rev Lett* 2014, 112:176802.

126. Lu W, Nan H, Hong J, Chen Y, Zhu C, Liang Z, Ma X, Ni Z, Jin C, Zhang Z. Plasma-assisted

fabrication of monolayer phosphorene and its Raman characterization. *Nano Res* 2014, 7:853–859.

127. Yasaei P, Kumar B, Foroozan T, Wang C, Asadi M, Tuschel D, Indacochea JE, Klie RF, Salehi-Khojin A. High-quality black phosphorus atomic layers by liquid-phase exfoliation. *Adv Mater* 2015, 27:1887–1892.
128. Brent JR, Savjani N, Lewis EA, Haigh SJ, Lewis DJ, O'Brien P. Production of few-layer phosphorene by liquid exfoliation of black phosphorus. *Chem Commun* 2014, 50:13338–13341.
129. Wang G, Pandey R, Karna SP. Effects of extrinsic point defects in phosphorene: B, C, N, O, and F adatoms. *Appl Phys Lett* 2015, 106:173104.
130. Kou L, Frauenheim T, Chen C. Phosphorene as a superior gas sensor: Selective adsorption and distinct I–V response. *J Phys Chem Lett* 2014, 5:2675–2681.
131. Utt KL, Rivero P, Mehboudi M, Harriss EO, Borunda MF, Pacheco SanJuan AA, Barraza-Lopez S. Intrinsic defects, fluctuations of the local shape, and the photo-oxidation of black phosphorus. *ACS Cent Sci* 2015, 1:320–327.
132. Watanabe K, Taniguchi T, Kanda H. Direct-bandgap properties and evidence for ultraviolet lasing of hexagonal boron nitride single crystal. *Nat Mater* 2004, 3:404–409.
133. Zhi C, Bando Y, Tang C, Kuwahara H, Golberg D. Large-scale fabrication of boron nitride nanosheets and their utilization in polymeric composites with improved thermal and mechanical properties. *Adv Mater* 2009, 21:2889–2893.
134. Grad G, Blaha P, Schwarz K, Auwärter W, Greber T. Density functional theory investigation of the geometric and spintronic structure of h-BN/Ni (111) in view of photoemission and STM experiments. *Phys Rev B* 2003, 68:085404.
135. Song L, Ci L, Lu H, Sorokin PB, Jin C, Ni J, Kvashnin AG, Kvashnin DG, Lou J, Yakobson BI. Large scale growth and characterization of atomic hexagonal boron nitride layers. *Nano Lett* 2010, 10:3209–3215.
136. Shi Y, Hamsen C, Jia X, Kim KK, Reina A, Hofmann M, Hsu AL, Zhang K, Li H, Juang Z-Y. Synthesis of few-layer hexagonal boron nitride thin film by chemical vapor deposition. *Nano Lett* 2010, 10:4134–4139.
137. Kim KK, Hsu A, Jia X, Kim SM, Shi Y, Hofmann M, Nezich D, Rodriguez-Nieva JF, Dresselhaus M, Palacios T. Synthesis of monolayer hexagonal boron nitride on Cu foil using chemical vapor deposition. *Nano Lett* 2011, 12:161–166.
138. Pacile D, Meyer J, Girit CO, Zettl A. The two-dimensional phase of boron nitride: few-atomic-layer sheets and suspended membranes. *Appl Phys Lett* 2008, 92:133107.
139. Lee C, Li Q, Kalb W, Liu X-Z, Berger H, Carpick RW, Hone J. Frictional characteristics of atomically thin sheets. *Science* 2010, 328:76–80.
140. Dean C, Young A, Meric I, Lee C, Wang L, Sorgenfrei S, Watanabe K, Taniguchi T, Kim P, Shepard K. Boron nitride substrates for high-quality graphene electronics. *Nat Nanotechnol* 2010, 5:722–726.
141. Li LH, Cervenka J, Watanabe K, Taniguchi T, Chen Y. Strong oxidation resistance of atomically thin boron nitride nanosheets. *ACS Nano* 2014, 8:1457–1462.
142. Chen Y, Zou J, Campbell SJ, Le Caer G. Boron nitride nanotubes: pronounced resistance to oxidation. *Appl Phys Lett* 2004, 84:2430–2432.
143. Yi M, Shen Z, Zhao X, Liang S, Liu L. Boron nitride nanosheets as oxygen-atom corrosion protective coatings. *Appl Phys Lett* 2014, 104:143101.
144. Chen Y, Hu C-L, Li J-Q, Jia G-X, Zhang Y-F. Theoretical study of O_2 adsorption and reactivity on single-walled boron nitride nanotubes. *Chem Phys Lett* 2007, 449:149–154.
145. Petravic M, Peter R, Kavre I, Li LH, Chen Y, Fan L-J, Yang Y-W. Decoration of nitrogen vacancies by oxygen atoms in boron nitride nanotubes. *Phys Chem Chem Phys* 2010, 12:15349–15353.
146. Gao M, Lyalin A, Taketsugu T. Oxygen activation and dissociation on h-BN supported Au atoms. *Int J Quantum Chem* 2013, 113:443–452.
147. Lyalin A, Nakayama A, Uosaki K, Taketsugu T. Functionalization of monolayer h-BN by a metal support for the oxygen reduction reaction. *J Phys Chem C* 2013, 117:21359–21370.
148. Si M, Xue D. Oxidation fracturing of the graphitic BN sheet. *J Phys Chem Solids* 2010, 71:1221–1224.
149. Wang QH, Kalantar-Zadeh K, Kis A, Coleman JN, Strano MS. Electronics and optoelectronics of two-dimensional transition metal dichalcogenides. *Nat Nanotechnol* 2012, 7:699–712.
150. Coleman JN, Lotya M, O'Neill A, Bergin SD, King PJ, Khan U, Young K, Gaucher A, De S, Smith RJ. Two-dimensional nanosheets produced by liquid exfoliation of layered materials. *Science* 2011, 331:568–571.
151. Ayari A, Cobas E, Ogundadegbe O, Fuhrer MS. Realization and electrical characterization of ultrathin crystals of layered transition-metal dichalcogenides. *J Appl Phys* 2007, 101:14507.
152. Chhowalla M, Shin HS, Eda G, Li L-J, Loh KP, Zhang H. The chemistry of two-dimensional layered transition metal dichalcogenide nanosheets. *Nat Chem* 2013, 5:263–275.
153. Kim IS, Sangwan VK, Jariwala D, Wood JD, Park S, Chen K-S, Shi F, Ruiz-Zepeda F, Ponce A, Jose-Yacaman M. Influence of stoichiometry on the optical

and electrical properties of chemical vapor deposition derived MoS_2. *ACS Nano* 2014, 8:10551–10558.

154. Kam K, Parkinson B. Detailed photocurrent spectroscopy of the semiconducting group VIB transition metal dichalcogenides. *J Phys Chem* 1982, 86:463–467.
155. Mak KF, Lee C, Hone J, Shan J, Heinz TF. Atomically thin MoS_2: a new direct-gap semiconductor. *Phys Rev Lett* 2010, 105:136805.
156. Novoselov K, Jiang D, Schedin F, Booth T, Khotkevich V, Morozov S, Geim A. Two-dimensional atomic crystals. *Proc Natl Acad Sci USA* 2005, 102:10451–10453.
157. Yoon Y, Ganapathi K, Salahuddin S. How good can monolayer MoS_2 transistors be? *Nano Lett* 2011, 11:3768–3773.
158. Ataca C, Sahin H, Ciraci S. Stable, single-layer MX_2 transition-metal oxides and dichalcogenides in a honeycomb-like structure. *J Phys Chem C* 2012, 116:8983–8999.
159. Li Y, Li Y-L, Araujo CM, Luo W, Ahuja R. Single-layer MoS_2 as an efficient photocatalyst. *Catal Sci Technol* 2013, 3:2214–2220.
160. Lopez-Sanchez O, Lembke D, Kayci M, Radenovic A, Kis A. Ultrasensitive photodetectors based on monolayer MoS_2. *Nat Nanotechnol* 2013, 8:497–501.
161. Zeng H, Dai J, Yao W, Xiao D, Cui X. Valley polarization in MoS_2 monolayers by optical pumping. *Nat Nanotechnol* 2012, 7:490–493.
162. Zhang W, Huang JK, Chen CH, Chang YH, Cheng YJ, Li LJ. High-gain phototransistors based on a CVD MoS_2 monolayer. *Adv Mater* 2013, 25:3456–3461.
163. Lee YH, Zhang XQ, Zhang W, Chang MT, Lin CT, Chang KD, Yu YC, Wang JTW, Chang CS, Li LJ. Synthesis of large-area MoS_2 atomic layers with chemical vapor deposition. *Adv Mater* 2012, 24:2320–2325.
164. Wang X, Feng H, Wu Y, Jiao L. Controlled synthesis of highly crystalline MoS_2 flakes by chemical vapor deposition. *J Am Chem Soc* 2013, 135:5304–5307.
165. Shaw JC, Zhou H, Chen Y, Weiss NO, Liu Y, Huang Y, Duan X. Chemical vapor deposition growth of monolayer $MoSe_2$ nanosheets. *Nano Res* 2014, 7:511–517.
166. Zhang D, Wang DZ-R, Creswell R, Lu C, Liou J, Herman IP. Passivation of CdSe quantum dots by graphene and MoS_2 monolayer encapsulation. *Chem Mater* 2015, 27:5032–5039.
167. Sen HS, Sahin H, Peeters F, Durgun E. Monolayers of MoS_2 as an oxidation protective nanocoating material. *J Appl Phys* 2014, 116:083508.
168. Wu J, Li H, Yin Z, Li H, Liu J, Cao X, Zhang Q, Zhang H. Layer thinning and etching of mechanically exfoliated MoS_2 nanosheets by thermal annealing in air. *Small* 2013, 9:3314–3319.
169. Kang N, Paudel HP, Leuenberger MN, Tetard L, Khondaker SI. Photoluminescence quenching in single-layer MoS_2 via oxygen plasma treatment. *J Phys Chem C* 2014, 118:21258–21263.
170. Zhou H, Yu F, Liu Y, Zou X, Cong C, Qiu C, Yu T, Yan Z, Shen X, Sun L. Thickness-dependent patterning of MoS2 sheets with well-oriented triangular pits by heating in air. *Nano Res* 2013, 6:703–711.
171. Ionescu R, George A, Ruiz I, Favors Z, Mutlu Z, Liu C, Ahmed K, Wu R, Jeong JS, Zavala L. Oxygen etching of thick MoS_2 films. *Chem Commun* 2014, 50:11226–11229.
172. Yamamoto M, Einstein TL, Fuhrer MS, Cullen WG. Anisotropic etching of atomically thin MoS_2. *J Phys Chem C* 2013, 117:25643–25649.